Nanoscale Res Lett (2009) 4:1–10
DOI 10.1007/s11671-008-9200-y

NANO REVIEW

Enhancing Solar Cell Efficiencies through 1-D Nanostructures

Kehan Yu · Junhong Chen

Received: 31 July 2008 / Accepted: 27 October 2008 / Published online: 25 November 2008

Abstract The current global energy problem can be attributed to insufficient fossil fuel supplies and excessive greenhouse gas emissions resulting from increasing fossil fuel consumption. The huge demand for clean energy potentially can be met by solar-to-electricity conversions. The large-scale use of solar energy is not occurring due to the high cost and inadequate efficiencies of existing solar cells. Nanostructured materials have offered new opportunities to design more efficient solar cells, particularly one-dimensional (1-D) nanomaterials for enhancing solar cell efficiencies. These 1-D nanostructures, including nanotubes, nanowires, and nanorods, offer significant opportunities to improve efficiencies of solar cells by facilitating photon absorption, electron transport, and electron collection; however, tremendous challenges must be conquered before the large-scale commercialization of such cells. This review specifically focuses on the use of 1-D nanostructures for enhancing solar cell efficiencies. Other nanostructured solar cells or solar cells based on bulk materials are not covered in this review. Major topics addressed include dye-sensitized solar cells, quantum-dot-sensitized solar cells, and p-n junction solar cells.

Keywords Solar cells · Nanowires · Nanotubes · Nanorods · Quantum dots · Hybrid nanostructures

K. Yu · J. Chen (✉)
Department of Mechanical Engineering, University of Wisconsin-Milwaukee, Milwaukee, WI 53211, USA
e-mail: jhchen@uwm.edu

Introduction

Energy supply has arguably become one of the most important problems facing humanity [1]. The exponential demand for energy is evidenced by dwindling fossil fuel supplies [2] and record-high oil and gas prices due to global population growth and economic development (Fig. 1) [3, 4]. This energy shortage has significant implications to the future of our society—for example, in order for 10 billion people to sustain their current lifestyle with their current energy consumption, we need a minimum of ten additional terawatts (TWs), an equivalent of 150 millions of barrels of oil per day (150 M BOE/Day), until the year 2050 [5]. The energy crisis is further exacerbated by major concerns about global warming from greenhouse gas emissions due to increasing fossil fuel consumption [6–8].

At this large scale, solar energy seems to be the most viable choice to meet our clean energy demand. The sun continuously delivers to the earth 120,000 TW of energy, which dramatically exceeds our current rate of energy needs (13 TW) [9]. This implies that covering only 0.1% of the earth's surface with solar cells of 10% efficiency would satisfy our current energy needs [10]; however, the energy currently produced from sunlight remains less than 0.1% of the global energy demand (Fig. 2, data from [11]). The major barrier for the large-scale use of solar energy is the high cost and inadequate efficiencies of existing solar cells. Innovations are needed to harvest incident solar photons with greater efficiency and economical viability [12, 13].

The best commercial solar cells based on single-crystal silicon are about 18% efficient [9, 14]. These conventional p-n junction cells, so-called first-generation devices, suffer from the high cost of manufacturing and installation. The second-generation devices consisting of $CuInGaSe_2$ (CIGS) polycrystalline semiconductor thin films can reduce the price

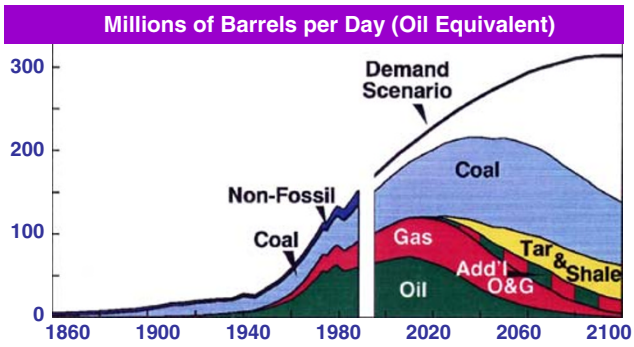

Fig. 1 Historical and projected world energy supply and demand (Reproduced from Ref. [4].)

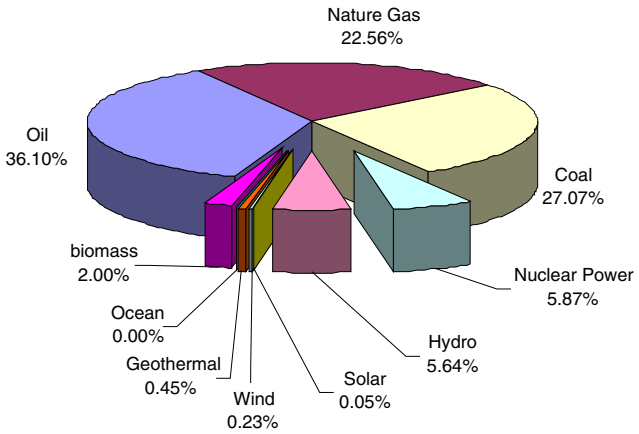

Fig. 2 Worldwide primary energy consumption by energy type (Data from Ref. [11]. Reproduced by permission of the MRS Bulletin.)

significantly, but it does not reduce the challenge to make their efficiencies more practical. Now the third-generation solar cells, such as dye-sensitized solar cells (DSSCs) [15, 16], bulk heterojunction cells [17–19], and organic cells [20], are promising for inexpensive and large-scale solar energy conversion (Table 1 [9]); however, laboratory DSSCs based on cheap dye sensitization of oxide semiconductors are typically less than 10% efficient, and those based on even cheaper organic materials are 2–5% efficient.

Nanostructured semiconductors, organic-inorganic hybrid assemblies, and molecular assemblies present new opportunities to design such third-generation light energy conversion devices. Considerable efforts have been devoted to the development of more efficient photoanode materials, such as ordered mesostructured materials [21] and one-dimensional (1-D) nanostructures (nanowires, nanotubes, and nanorods) [22–24]. Examples of 1-D nanostructures include highly ordered TiO_2 nanotube arrays synthesized with anodization of Ti foils, ZnO nanowire arrays synthesized with aqueous solutions, and carbon nanotube (CNT) and Si nanowire arrays synthesized with chemical vapor deposition (CVD) [23–34]. Bandgap-tunable semiconductor zero-dimensional (0-D) nanomaterials, such as CdS [35–37], PbS [38, 39], Bi_2S_3 [38, 40], CdSe [41], and InP [42] quantum dots (QDs), have demonstrated extraordinary optical and electronic properties that open up possibilities for revolutionary advances in photovoltaic (PV) devices. The combination of 1-D with 0-D nanostructures is attracting more interests from the solar cell community. Assembly methods for these hybrid nanostructures include wet-chemistry processes through chemical functionalization [43–47] and dry routes through the electrostatic-force-directed assembly [48, 49].

In particular, 1-D nanostructures are promising for photovoltaic devices due to several performance and processing benefits, such as a direct path for charge transport and large surface areas for light harvest offered by the geometry of such nanostructures. For example, the mobility of electrons in 1-D nanostructures is typically several orders of magnitude higher than that in semiconductor nanoparticle films commonly used in DSSCs (Table 2, data from [23, 50–54]). This review addresses some of the current research issues in the field of new solar cells based on 1-D semiconductor nanostructures, and hybrids of 1-D nanomaterials and dye molecules or QDs. These solar cells include DSSCs with TiO_2 nanotube or ZnO nanowire arrays as photoanodes in lieu of nanoparticle networks, solar cells with tunable-bandgap QDs supported by wide-bandgap semiconductor nanotube/nanowire or CNT arrays, and solar cells with coaxial p-n junctions in vertically-aligned 1-D nanostructures or p-n junctions between the 1-D nanostructure and the substrate. We summarize recent advances and discuss the performance and properties of these innovative solar energy harvesting and conversion devices.

Dye-Sensitized Solar Cells

A dye-sensitized solar cell (DSSC) is a type of photoelectrochemical (PEC) solar cell which has been studied extensively [55–57]. In a DSSC, dye molecules are used to sensitize wide-bandgap semiconductors, such as TiO_2 and ZnO, which assist in separating electrons from photoexcited dye molecules. The visible light absorbed by dye molecules is more intensive than the UV light absorbed by wide-bandgap semiconductors for solar radiation, even if the energy of visible light is lower than that of UV light. The sensitization of wide-bandgap semiconductors by adsorbed monolayers of dye molecules began in the late 1960s with the work of Gerishcer [58] and Memming [59]. A conceptual and practical breakthrough occurred in the late 1980s when Grätzel and coworkers started using high-surface-area semiconductors for DSSCs [16, 60–63]. A schematic representation of a DSSC is shown in Fig. 3 [64]. Its working principle is: (1) The incident photon is

Table 1 Photovoltaic conversion efficiencies (Reprinted with permission from Ref. [9]. Copyright 2007, American Institute of Physics.)

	Laboratory best (%)	Thermodynamic limit (%)
Single junction		31
Silicon (crystalline)	25	
Silicon (nanocrystalline)	10	
Gallium arsenide	25	
Dye-sensitized	10	
Organic	5	
Multijunction	32	66
Concentrated sunlight (single junction)	28	41
Carrier multiplication		42

Table 2 Comparison of electron mobilities ($cm^2\ V^{-1}\ s^{-1}$) of 1-D nanomaterials and nanoparticles

Nanomaterials	Electron mobilities ($cm^2\ V^{-1}\ s^{-1}$)
SWCNT	7.9[a]–$10^{b} \times 10^4$
Si nanowire	1000[c]
Ge nanowire	600–700[d]
ZnO nanowire	1–5[e]
ZnO nanoparticle film	0.017–0.066[f]
TiO_2 nanoparticle film	$<10^{-3}$[g]

[a] Field-effect and; [b] intrinsic mobility of a 300 nm long and 3.9 nm diameter single-walled carbon nanotube (SWCNT) [50]; [c] 8–30 nm wide Si nanowires [51]; [d] 20 nm wide Ge nanowires [52]; [e] 16–17 μm long and 130–200 nm wide ZnO nanowire [23]; [f] for particle size around 4 nm [53]; [g] for 4–8 nm anatase TiO_2 nanocrystals; it is 15 $cm^2\ V^{-1}\ s^{-1}$ in single crystal TiO_2 [54]

absorbed by the dye molecule adsorbed on the surface of nanocrystalline TiO_2 particles and an electron from the molecular ground state S^0 is excited to an excited state S*; (2) The excited electron of the dye is injected into the conduction band of the TiO_2 particles, leaving the dye molecule to an oxidized state S^+; (3) The injected electron percolates through the porous nanocrystalline structure to the transparent conducting oxide (TCO) layer of the glass substrate (negative electrode or anode) and finally through an external load to the counter electrode (positive electrode or cathode); (4) At the counter electrode, the electron is transferred to the triiodide (I_3^-) in electrolyte to yield iodide (I^-); (5) The cycle is closed through reducing the oxidized dye by the iodide in the electrolyte. However, there is no net chemistry in terms of chemicals created or destroyed in the device, so the cell is regenerative.

The anodes of DSSCs are typically constructed with a thin film (~10 μm) of wide bandgap semiconductor nanoparticles involving SnO_2 [65], ZnO [66, 67], or TiO_2

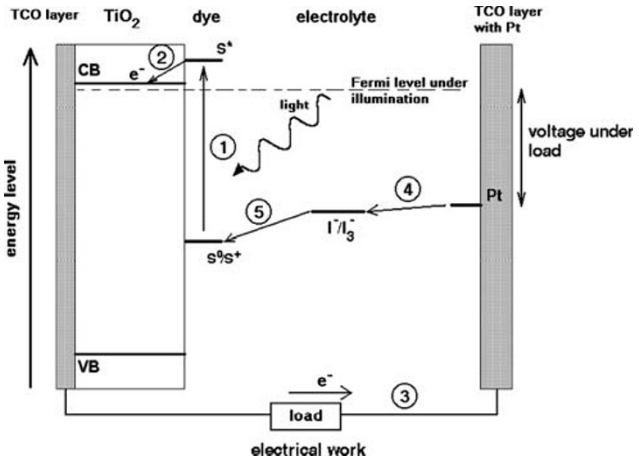

Fig. 3 The working principle of a dye-sensitized nanostructure solar cell (Adapted from Ref. [64])

[68–74]. The nanoparticle film provides a large surface (~1000 times higher than the geometrical area of the electrode) for absorption of light-harvesting molecules (usually ruthenium-based dyes); however, electrons are usually trapped by isolated nanoparticles, surface states, or defect states. The so-called trap effects slow down the electron transport through diffusion and limit the device efficiency, which has been proved by time-resolved photocurrent and photovoltage measurements [75, 76] and modeling studies [77, 78]. Under full sunlight, the average injected electron may experience a million trapping events before either being collected by the electrode or recombining with an oxidizing species [79]. Electron transport speed in single crystals is much larger than that in polycrystalline nanocrystals. For example, electron transport in crystalline wires is expected to be several orders of magnitude faster than percolation through a random polycrystalline network (Table 2). 1-D wide-bandgap semiconductor nanostructures were thus introduced to improve the charge collection.

Crystalline ZnO nanowire arrays were introduced to replace the traditional nanoparticle anode [23, 80]. Electric properties of individual nanowires were studied by Law et al. [23]. The ZnO nanowire array of high surface area was synthesized using a simple two-step process in aqueous solutions. Briefly, a 10–15-nm-thick film of ZnO quantum dots was deposited onto fluorine-doped tin oxide (FTO) conductive glass substrates by dip coating, and wires were then grown from these nuclei through thermal decomposition of a zinc complex. Individual ZnO nanowire resistivity varied from 0.3 to 2.0 Ω cm, with an electron concentration of 1–5 × 10^{18} cm^{-3} and mobility (μ) of 1–5 $cm^2\ V^{-1}\ s^{-1}$. Using the Einstein relation, $D = k_B T\mu/e$, an electron diffusivity D_n = 0.05–0.5 $cm^2\ s^{-1}$ for a single nanowire can be estimated. Compared with ZnO nanoparticles ($D_n \leq 10^{-4}\ cm^2\ s^{-1}$), the nanowire array

anode can collect charge carriers much more effectively by introducing highly ordered architectures. The electron injection rate can be investigated by transient mid-infrared absorption. Law et al. showed that the injection process in nanowires is complete after ~5 ps, but continues for ~100 ps in the nanoparticles [23]. The new cell exhibited a short-circuit current density $J_{sc} = 5.3–5.85$ mA/cm^2, an open-circuit voltage $V_{oc} = 0.61–0.71$ V, a fill factor FF = 0.36–0.38, and an efficiency $\eta = 1.2–1.5\%$ under AM1.5 sun illumination (100 ± 3 mW/cm^2). The external quantum efficiency of these cells peaks at 40–43% near the absorption maximum of the dye and is limited primarily by the relatively low dye loading of the nanowire film.

Analogous to ZnO nanowire arrays, well-aligned, self-organized TiO_2 nanotubes have been fabricated with the goal to improve electron transport pathways for solar energy conversion devices [24, 29, 30, 81–83]. Even though the efficiencies of these devices are not as high as cells fabricated with standard TiO_2 nanoparticles, respectable performance has been demonstrated. TiO_2 nanotube arrays allow direct charge transport along the length of the nanotube toward the electrode; however, this assumes that the charge transport in mesoporous TiO_2 is limited by interparticle traps. The advantage of nanorod or nanotube arrays will not be apparent if the surface trapping limits the charge transport [84]. Comparison between these 1-D nanostructures and standard films fabricated from sintered nanoparticles may very well assist in elucidating the mechanism for electron transport in these materials.

Recently, highly ordered TiO_2 nanotube arrays were synthesized by anodic oxidation of titanium and have generated considerable scientific interest [24–32]. To fabricate nanotube devices, titanium foil is anodized to achieve ordered nanopores. These nanopores initially have an amorphous structure, which can be transformed to anatase TiO_2 upon annealing to over 450 °C [85]. The porous film forms on the titanium foil and a compact titanium dioxide layer forms between the unoxidized titanium and the nanotubes during the heating process. Paulose et al. reported high open-circuit voltages of up to 860 mV for this cell structure [29]. Their best cells reached efficiencies of over 4% under AM1.5 Sun (iodide/triiodide-based cells). The nanotube devices display inhibited recombination characteristics with longer electron lifetimes, indicating fewer recombination centers in the nanotube film compared with a nanoparticle film [24].

A disadvantage of using TiO_2 nanotube arrays for anode fabrication is that the device requires illumination from the "back side" (through the Pt cathode) [86] because the counter electrode fabricated from Ti is opaque. This is not the optimal configuration for DSSCs because the platinum counter electrode partially reflects light and the iodine in the electrolyte absorbs photons at lower wavelengths. Therefore, the challenge is to achieve highly ordered TiO_2 nanotube arrays on FTO substrates, especially nanotubes with increased film thickness [30]. These are technical challenges that are likely to be solved in the near future.

Taking advantage of extremely high electron mobilities of single-walled CNTs (SWCNTs), Brown et al. deposited TiO_2 nanoparticles on an SWCNT network [87]. When modified with a sensitizer such as Ru(II)(bpy)^2(dcbpy), the SWCNT/TiO_2 film provided an unnoticeable influence on the charge injection from dye molecules into TiO_2 nanoparticles, but improved charge separation according to transient absorption and emission measurements. The rate of the back electron transfer between the oxidized sensitizer (Ru(III)) and TiO_2 was slower in the presence of the SWCNT scaffold. The incident photon to charge carrier efficiency (IPCE) at all wavelengths was enhanced by a factor of ~1.4 as a result of introducing a SWCNT scaffold in the mesoscopic TiO_2 film. This is due to the suppressed back electron transfer and the improved electron transport within the nanostructured TiO_2 film. However, the improvement in photocurrent generation was neutralized by a lower photovoltage, as the apparent Fermi level of the TiO_2 and SWCNT composite became more positive than that of pristine TiO_2. The dye-sensitized SWCNT/TiO_2 cell had $\eta = 0.13\%$, $V_{oc} = 0.26$ V, and $J_{sc} = 1.8$ mA/cm^2.

It is not surprising that the semiconductor nanotube/nanowire arrays are not always highly ordered, however. For instance, clumps of nanotubes and crack-like features in the films prepared by electrochemically anodizing titanium metal have been observed [26, 88]. The formation of clusters of bundled nanotubes in nominally oriented arrays could adversely affect the transport and recombination dynamics in TiO_2 films. Clusters of bundled nanotubes could be produced during the anodization process [26, 88] or during the cleaning and evaporative drying process of the as-grown films through capillary forces of the liquid acting between the nanotubes. Such capillary forces have the potential to not only bundle nanotubes but also to crack the film.

Removing liquids from the mesopores of the arrays by the supercritical CO_2 ($scCO_2$) drying technique can yield bundle-free and crack-free nanotube films. Compared with H_2O/air-dried TiO_2 nanotube array film, Zhu et al. found that the ethanol/$scCO_2$-dried films could prevent morphological disorders induced by capillary stress and enhance the total surface area of a film accessible to dye molecules by 23% [89]. The electron transport was about twice as fast in the ethanol/$scCO_2$-dried film than in the H_2O/air-dried film. The photoresponse of the DSSC with ordered films exhibited $J_{sc} = 5.7$ mA/cm^2, $V_{oc} = 0.58$ V, and FF = 0.56 to offer a solar conversion efficiency $\eta = 1.9\%$. In contrast, the DSSC with less-ordered films showed a J_{sc} of

4.9 mA/cm^2, V_{oc} of 0.60 V, and an FF of 0.53 to yield $\eta = 1.6\%$.

In general, DSSCs are relatively well developed in recent years with the following possible improvements. The growth of TiO_2 nanotube arrays on a transparent anode will be beneficial for the light absorption. A compact TiO_2 particle film between the FTO anode and the electrolyte was recently proved to reduce charge recombination losses [74], which might be a valuable hint to design TiO_2 nanotube array for DSSCs. Use of bundle-free and crack-free 1-D nanostructure arrays is another principle for solar cell assembly. High aspect ratio nanotube/nanowire arrays are expected to load more dye molecules, but the dilemma is that tubes/wires longer than the diffusion length of electrons will degrade the efficiency of electron collection. Recent work also includes the molecular engineering of suitable ruthenium compounds, which are known for their excellent stability [90]. The use of solvent-free electrolytes such as ionic liquids has made striking advances during the past few years [91, 92]. These nonvolatile redox melts show great promise for use in outdoor photovoltaic systems and have been discussed in detail elsewhere [93].

Quantum-Dot-Sensitized Solar Cells

The combination of two or more nanostructure architectures provides another option to modulate the performance of light-harvesting devices [94–97]. As presented in the previous section, the electron transport across particles is susceptible to recombination loss at the grain boundaries and charge trapping in nanostructured semiconductor films prepared from particles. The use of nanotube/nanowire support to anchor light-harvesting assemblies (e.g., semiconductor particles and dye molecules) provides a convenient way to capture photogenerated charges and transport them to electrodes. Quantum-dot-sensitized solar cells (QDSSCs) provide additional opportunities that are not available with dye-sensitized solar cells (Fig. 4 [98]). First, the use of quantum dots in lieu of the dye molecules provides the ability to tune the optical absorption in the solar cell through selection of semiconductor material and particle size. Second, QDSSCs can potentially exploit the recently observed multiple electron-hole pair generation per photon to achieve higher efficiencies [99, 100] than that predicted by Shockley and Queisser [101].

A SWCNT is an ideal channel for collecting and transporting charges across light-harvesting assemblies. Significant progress has been achieved in synthesizing semiconductor-CNT composite films in recent years [102–109]. These earlier studies have mainly focused on establishing synthetic strategies and characterizing the composite systems, including CNTs with TiO_2 [110], SnO_2 [111], CdSe [106, 108], and CdS [112] nanocrystals. Most of the wet-chemistry strategies involve chemical functionalization of the CNT surface followed by the assembly of nanocrystals onto the CNTs via covalent [43], noncovalent [44], or electrostatic interactions [45, 46]. For example, the CdS QDs can be deposited on SWCNTs with chemical methods [47]. SWCNTs were dispersed in tetrahydrofuran (THF) with the aid of tetraoctylammonium bromide (TOAB). The adsorption of Cd^{2+} ions on the SWCNT surface followed by reaction with S^{2-} provides a simple and convenient method of preparing SWCNT–CdS composites. The CdS-SWCNT composite is capable of generating a photocurrent from visible light with unusually high efficiencies [47, 103], in which the luminescence of CdS is quenched by SWCNT. Transient absorption experiments have confirmed the quick deactivation of excited CdS on the SWCNT surfaces, as the transient bleaching recovers in about 200 ps. The ability of the CdS-SWCNT nanocomposite system to undergo photo-induced charge separation opens up new ways to design light-harvesting assemblies [5].

Although the wet-chemistry methods work well with randomly dispersed CNTs, they are not suitable for vertically aligned CNTs. The aligned structure will be damaged in the wet processing because the upper ends of the neighboring nanotubes have been seen to bundle together and cause some nanotubes to lay down [113]. Chen et al. have recently developed a material-independent dry route based on the electrostatic-force-directed assembly (ESFDA) to

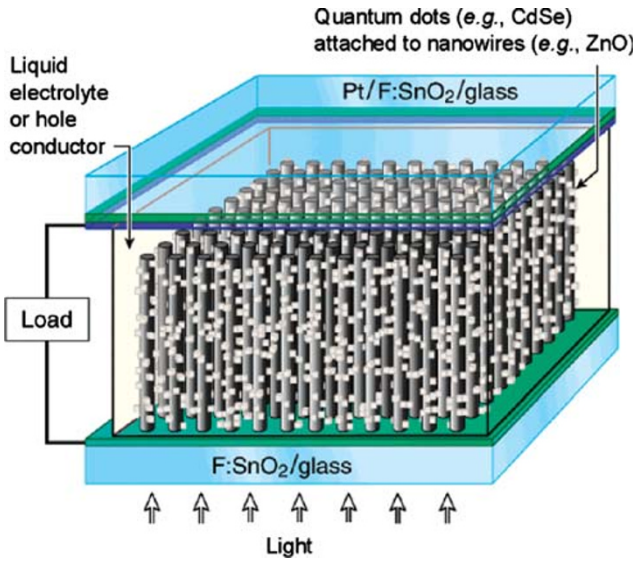

Fig. 4 Schematic of a quantum-dot-sensitized solar cell (QDSSC). An array of ZnO nanowires, grown vertically from an FTO/glass substrate and decorated with CdSe quantum dots, serves as the photoanode. A second FTO/glass substrate, coated with a 100 Å layer of Pt, is the photocathode. The space between the two electrodes is filled with a liquid electrolyte and the cell is illuminated from the bottom (Reprinted with permission from Ref. [98]. Copyright 2007, American Chemical Society.)

assemble aerosol nanocrystals onto CNTs [48, 49]. In principle, the ESFDA technique works for both random CNTs and aligned CNTs without the need for chemical functionalization or other pretreatments of the CNTs. In ESFDA, charged and nonagglomerated aerosol nanocrystals were produced from a mini-arc plasma source and then delivered to the electrically biased CNTs in an inert carrier gas [114]. The electric field near the CNT surface was enhanced significantly and the aerosol nanocrystals were attracted to the external surface of the CNTs. With this technique, Chen et al. have demonstrated the successful assembly of various nanocrystals, including single-component nanocrystals (Au, Ag, and SnO_2) [48, 115] and multicomponent nanocrystals (SnO_2 and Ag) [115], onto randomly dispersed multiwalled CNTs (MWCNTs), SWCNTs, and vertically aligned MWCNTs [48, 49].

The highly ordered charge transport channel is not limited to only CNTs, but also to other semiconductor (ZnO [98] or TiO_2 [97]) 1-D nanostructures. Quantum-dot-sensitized nanowire solar cell based on photosensitization of ZnO nanowires with CdSe quantum dots has been demonstrated [98]. A ZnO nanowire array can be grown directly onto transparent and conducting FTO substrates from an aqueous solution of $Zn(NO_3)_2$ and methenamine between 80 and 95 °C [23, 116, 117]. CdSe QDs were assembled on the ZnO nanowires by using bifunctional molecules of the type X-R-Y, where X and Y are groups that bind to CdSe (X = –SH) and ZnO (Y = –COOH), respectively. The photocurrent is generated from visible light by the excitation of electron-hole pairs in the CdSe QDs. The electrons are injected across the QD-nanowire interface into the ZnO, a process that is facilitated by the overlap between the electronic states in the QD and the ZnO conduction band. The morphology of the nanowires provides the photoinjected electrons with a direct electrical pathway to the photoanode. The ZnO nanowire-based QDSSCs exhibited $\eta = 0.4\%$, $V_{oc} = 0.5$–0.6 V, $J_{sc} =$ 1–2 mA/cm^2, and a fill factor FF ~ 0.3.

TiO_2 is another important wide-bandgap semiconductor that is widely used in both DSSCs and QDSSCs. Sun et al. reported an investigation on the CdS QDs sensitized TiO_2 nanotube array photoelectrodes and their performance in photoelectrochemical solar cells [97]. The highly ordered TiO_2 nanotube films were synthesized by anodic oxidation in a NH_4F organic electrolyte. The CdS QDs were deposited into the crystalline TiO_2 nanotubes by the sequential chemical bath deposition method. The CdS-TiO_2 cells exhibited impressive $\eta = 4.15$ %, $V_{oc} = 1.27$ V, $J_{sc} =$ 7.82 mA/cm^2, and FF = 0.578 under AM1.5 illuminations. These results clearly demonstrated that significant improvement on the PEC cell efficiency can be obtained via incorporating inorganic semiconductor QDs into the TiO_2 nanotube array films.

A number of active research areas could significantly contribute to the advancement of QDSSCs. Maximizing the overlap between the solar spectrum and the solar cell absorption spectrum through judiciously selecting tunable-bandgap QDs is an ongoing effort. The multiple exciton generation with UV photons demonstrated in QDs is yet to be proved in solar cells. The challenge is to find ways to effectively collect the resulting excitons before they recombine since recombination occurs at a femtosecond time scale. Assembling QDs onto nanotubes/nanowires with wet-chemistry methods will likely damage the ordered arrays, and molecule linkers between QDs and 1-D nanostructures are likely to be potential barriers for charge transfer. Dry methods such as ESFDA could potentially achieve better electronic transfer between QDs and 1-D nanostructures. Use of Fe or Ni as catalysts in CVD growth of CNTs constrains the material types of substrates and makes it difficult to achieve Ohmic contacts between CNTs and substrates. More understanding on the electronic transfer at the QDs-nanotubes/nanowires heterojunction interface and CNTs-substrate interface is imperative to further improve the performance of QDSSCs.

1-D Nanostructure Solar Cells

Many researchers have been eager to explore carbon nanostructures such as SWCNT assemblies for energy conversion devices because of their unique electrical and electronic properties, wide electrochemical stability window, and high surface area [118–120]. Fullerenes, for example, exhibit rich photochemistry and act as an electron shuttle in photochemical solar cells [121]. They also play an important role in improving the performance of organic photovoltaic cells. On the other hand, the semiconducting CNTs undergo charge separation when subjected to band-gap excitation. The exciton annihilation and charge separation processes have been characterized by transient absorption and emission measurements [5].

For example, the photoresponse of CNT filaments was realized in early years from the elastic response of the aligned bundles between two metal electrodes [122]. Hot carrier luminescence from ambipolar CNT field-effect transistors (FETs) has been monitored by Avouris and coworkers [123]. The relaxation of electrons and holes to the fundamental band edge occurs within 100 fs after photoexcitation [124]. These early studies confirmed the ability of CNTs to possess a band structure that can undergo electron-hole charge separation with visible light excitation.

It is important that photoinduced charge carriers are separated before recombination to generate electricity. However, spatially confined charge carriers in the nanotube

are bound by Coulombic interactions with the bound pair referred to as an exciton [125–127]. A small fraction of the excitons are able to dissociate and form unbounded electron-hole (e-h) pairs [124]. Accordingly, the dissociation of excitons becomes an important process for photocurrent generation. A key question is whether the photoinduced charge carriers generated in SWCNTs can be collected suitably for photocurrent generation, similar to the photovoltaic application of other semiconductors [128].

Double-walled carbon nanotubes (DWCNTs) were also directly configured as energy conversion materials to fabricate thin film solar cells, with nanotubes serving as both photogeneration sites and a charge carriers collecting/transport layer [129]. The solar cells consisted of a semitransparent thin film of nanotubes conformally coated on an n-type crystalline silicon substrate to create high-density p-n heterojunctions between nanotubes and n-Si to favor charge separation and extract electrons (through n-Si) and holes (through nanotubes). The p-type DWCNTs were first formed as an ultrathin film on the water surface with the aid of ethanol, and then transferred to an n-Si substrate. Experiments have shown $\eta = 1.38\%$, $V_{oc} = 0.5$ V, $J_{sc} = 13.8$ mA/cm^2, and FF = 19% under AM1.5 illumination, proving that DWCNTs-on-Si is a potentially suitable configuration for solar cells.

The 1-D nanostructure also promotes traditional p-n junction solar cell performance. Two key constraints for this type of solar cell are (1) the material must be sufficiently thick and pure to absorb most of the solar photons with energies above the material's bandgap; and (2) the material must have a high minority carrier diffusion length to effectively collect the photogenerated charge carriers. One attractive method to improve the light absorption and charge carrier collection involves high aspect ratio cylindrical absorbers, such as 1-D nanowires [130]. A preferred implementation includes the use of wires that are sufficiently long to absorb most of the incident light and have sufficiently small diameters to facilitate efficient radial collection of carriers, even for relatively impure absorber materials (Fig. 5 [131]). To fabricate such a solar cell, methods are required (1) to prepare large area arrays of vertically aligned core-shell nanowires; (2) to make electrical junctions to such wire arrays; and (3) to make electrical contacts to the backsides of these devices. These challenges have been investigated by various means, including chemical vapor deposition (CVD) growth of wire arrays [33, 34], etching of flat substrates to produce wire arrays [132, 133], and creating conductive polymer electrical junctions with wires [19, 134].

In an earlier theoretical work by Kayes et al., a device physics model has been developed for radial p-n junction nanowire/nanorod solar cells, in which densely packed nanorods, each having a p-n junction in the radial direction, are oriented with the rod axis parallel to the incident light direction [131]. The radial p-n junction nanorod geometry produces significant improvements in the efficiencies of cells made from materials that have diffusion lengths at least two orders of magnitude less than their optical thickness and low recombination in the depletion region (for example, exciton lifetime $> \sim 10$ ns for silicon). Optimal cells have a radius approximately equal to the minority-electron diffusion length in the p-type core, and their doping levels must be high enough that a rod of such radius is not fully depleted. In silicon with very low diffusion lengths (L_n = 100 nm), extremely large efficiency gains (from 1.5% to 11%) are possible by exploiting the radial p-n junction nanorod geometry, provided that the trap density in the depletion region remains fixed at a relatively low level ($< \sim 3 \times 10^{15}$ cm^{-3}).

Maiolo et al. experimentally showed that optimal efficiencies can be obtained when the Si wires have a diameter comparable to the minority carrier diffusion length [131, 135]. Smaller diameters increase the surface area, thereby increasing the surface and junction recombination with few accompanying improvements in carrier collection. Based on the study of Kayes et al., Tsakalakos et al. also estimated an efficiency of 15–18% for Si nanowire solar cells [130]. According to the calculation, the lateral diffusion of minority carriers to the p-n junction, which is at most 50–500 nm away, was proposed rather than many microns away as in bulk Si solar cells. An array of Si nanowires (diameter = 189 ± 30 nm, length ~16 μm) was fabricated with CVD. A current density of ~1.6 mA/cm^2 for 1.8 cm^2 cells was obtained, and a broad external quantum

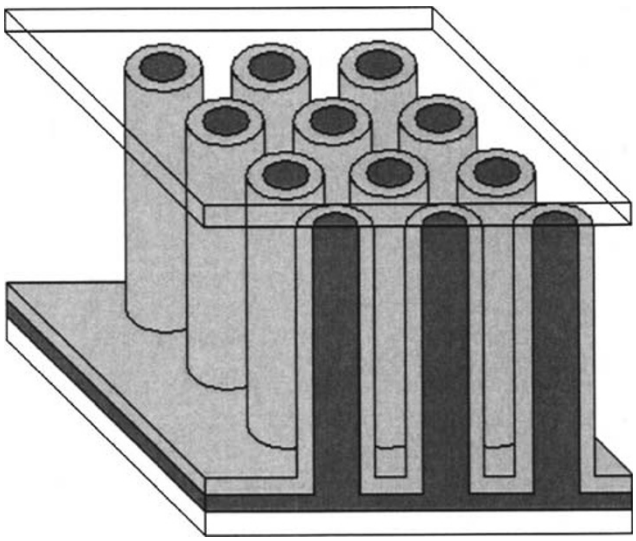

Fig. 5 Schematic cross section of a radial p-n junction core-shell nanowire solar cell. Light is incident on the top surface. The light gray area is n type; the dark gray area is p type (Reused with permission from Ref. [131]. Copyright 2005, American Institute of Physics.)

efficiency was measured with a maximum value of ~12% at 690 nm. The optical reflectance of the silicon nanowire solar cells was reduced by one to two orders of magnitude compared with planar cells.

Significant efforts are needed in the pursuit of 1-D nanostructure solar cells. Growth of 1-D nanostructures with higher electron mobility is always a direction of research. The junction area of a CNTs/Si cell is no more than the surface area of the anode (Si substrate). Therefore, rough architectures rather than planar ones are expected to improve the junction areas. Semiconductor nanowire/nanorods with radial p-n junctions make it possible to orthogonalize the direction of light absorption and carrier collection, and thus can enable efficient carrier collection in optically thick nanowire arrays even when minority carrier diffusion lengths are shorter than the optical absorption length. Although coaxial Si nanowire/nanorod p-n junction solar cells have high theoretical efficiencies, the cost of CVD growth of Si nanowires on Si substrates is high. Au as a catalyst used in the CVD growth of Si nanowire arrays also reduces the lifetime of carriers in silicon due to the presence of Au in the nanowire. Identifying inexpensive catalysts such as Cu has been demonstrated [136].

Conclusion

The sun provides enormous potential in helping to resolve the growing demand for energy worldwide; however, the high costs of implementing solar energy is a significant barrier compared with traditional energy sources, such as fossil fuels. The cost of a photovoltaic system is directly related to the low conversion efficiency, diluted energy density of solar radiation, and costly materials and fabrication process. During the past decade, the development of nanoscience and nanotechnology has launched new ways to design efficient solar cells. Strategies have been developed to design nanostructure architectures of semiconductors, metals, and polymers for solar cells. Theoretical and modeling studies have also helped to understand the optical and electrical processes of the photovoltaic conversion. The examples discussed in this review summarized how 1-D nanostructures, hybrids of 1-D nanomaterials/molecules, and QDs could aid in DSSCs, QDSSCs, and conventional p-n junction solar cells. While the new generation of photovoltaic cells offers many opportunities, it also presents challenges such as in the following directions (1) ordered assemblies of two or more nanocomponents on electrode surfaces; (2) new sensitizers or semiconductor systems that can harvest infrared photons; and (3) multiple exciton generation in semiconductor QDs. Worldwide, solar power is the star attraction for venture capitalists due to its booming laboratory research and commercialization. Although other forms of renewable energy can make significant contributions to current markets, sunlight is most available in the amount required to substitute completely for the energy quantities currently derived from hydrocarbons.

Acknowledgment This work was financially supported by the National Science Foundation through an NER grant (CMMI-0609059).

References

1. R.E. Smalley, MRS Bull **30**, 412 (2005)
2. P.B. Weisz, Phys. Today **57**, 47 (2004)
3. R.E. Smalley, Our energy challenge. http://smalley.rice.edu/ (2003)
4. J.F. Bookout, Episodes **12**, 257 (1989)
5. P.V. Kamat, J. Phys. Chem. C **111**, 2834 (2007)
6. C.D. Keeling, T.P. Whorf, M. Wahlen, J. Vanderplicht, Nature **375**, 666 (1995)
7. M.E. Mann, R.S. Bradley, M.K. Hughes, P.D. Jones, Science **280**, 2029 (1998)
8. DOE Argonne National Laboratory, Basic research needs for the hydrogen economy, Report of DOE BES workshop on hydrogen production, storage, and use, 13–15 May 2003
9. G.W. Crabtree, N.S. Lewis, Phys. Today **60**, 37 (2007)
10. M. Gratzel, Inorg. Chem. **44**, 6841 (2005)
11. R.E.H. Sims, MRS Bull. **33**, 389 (2008)
12. M.A. Green, *Third Generation Photovoltaics: Advanced Solar Energy Conversion* (Springer, Berlin, Germany, 2004)
13. K.W.J. Barnham, M. Mazzer, B. Clive, Nat. Mater. **5**, 161 (2006)
14. Basic research needs for solar energy utilization: Report of the BASIC Energy Sciences Workshop on Solar Energy Utilization, ed. by N.S. Lewis, G.W. Crabtree (US Department of Energy Office of Basic Energy Sciences, 2005)
15. U. Bach, D. Lupo, P. Comte, J.E. Moser, F. Weissortel, J. Salbeck, H. Spreitzer, M. Gratzel, Nature **395**, 583 (1998)
16. B. O'Regan, M. Gratzel, Nature **353**, 737 (1991)
17. G. Yu, J. Gao, J.C. Hummelen, F. Wudl, A.J. Heeger, Science **270**, 1789 (1995)
18. M.W. Rowell, M.A. Topinka, M.D. McGehee, H.J. Prall, G. Dennler, N.S. Sariciftci, L.B. Hu, G. Gruner, Appl. Phys. Lett. **88**, 233506 (2006)
19. W.U. Huynh, J.J. Dittmer, A.P. Alivisatos, Science **295**, 2425 (2002)
20. J. van de Lagemaat, T.M. Barnes, G. Rumbles, S.E. Shaheen, T.J. Coutts, C. Weeks, I. Levitsky, J. Peltola, P. Glatkowski, Appl. Phys. Lett. **88**, 233503 (2006)
21. M. Zukalova, A. Zukal, L. Kavan, M.K. Nazeeruddin, P. Liska, M. Gratzel, Nano Lett. **5**, 1789 (2005)
22. M. Adachi, Y. Murata, J. Takao, J.T. Jiu, M. Sakamoto, F.M. Wang, J. Am. Chem. Soc. **126**, 14943 (2004)
23. M. Law, L.E. Greene, J.C. Johnson, R. Saykally, P.D. Yang, Nat. Mater. **4**, 455 (2005)
24. K. Zhu, N.R. Neale, A. Miedaner, A.J. Frank, Nano Lett. **7**, 69 (2007)
25. S. Funk, B. Hokkanen, U. Burghaus, A. Ghicov, P. Schmuki, Nano Lett. **7**, 1091 (2007)
26. C.M. Ruan, M. Paulose, O.K. Varghese, G.K. Mor, C.A. Grimes, J. Phys. Chem. B **109**, 15754 (2005)

27. J.M. Macak, H. Tsuchiya, P. Schmuki, Angew. Chem. Int. Ed. **44**, 2100 (2005)
28. J.M. Macak, H. Tsuchiya, L. Taveira, S. Aldabergerova, P. Schmuki, Angew. Chem. Int. Ed. **44**, 7463 (2005)
29. M. Paulose, K. Shankar, O.K. Varghese, G.K. Mor, B. Hardin, C.A. Grimes, Nanotechnology **17**, 1446 (2006)
30. G.K. Mor, K. Shankar, M. Paulose, O.K. Varghese, C.A. Grimes, Nano Lett. **6**, 215 (2006)
31. S.P. Albu, A. Ghicov, J.M. Macak, R. Hahn, P. Schmuki, Nano Lett. **7**, 1286 (2007)
32. J. Park, S. Bauer, K. von der Mark, P. Schmuki, Nano Lett. **7**, 1686 (2007)
33. H.J. Fan, P. Werner, M. Zacharias, Small **2**, 700 (2006)
34. I. Lombardi, A.I. Hochbaum, P.D. Yang, C. Carraro, R. Maboudian, Chem. Mater. **18**, 988 (2006)
35. H. Gerischer, M. Lubke, J. Electroanal. Chem. **204**, 225 (1986)
36. R. Vogel, K. Pohl, H. Weller, Chem. Phys. Lett. **174**, 241 (1990)
37. S. Kohtani, A. Kudo, T. Sakata, Chem. Phys. Lett. **206**, 166 (1993)
38. R. Vogel, P. Hoyer, H. Weller, J. Phys. Chem. **98**, 3183 (1994)
39. R. Plass, S. Pelet, J. Krueger, M. Gratzel, U. Bach, J. Phys. Chem. B **106**, 7578 (2002)
40. L.M. Peter, K.G.U. Wijayantha, D.J. Riley, J.P. Waggett, J. Phys. Chem. B **107**, 8378 (2003)
41. D. Liu, P.V. Kamat, J. Phys. Chem. **97**, 10769 (1993)
42. A. Zaban, O.I. Micic, B.A. Gregg, A.J. Nozik, Langmuir **14**, 3153 (1998)
43. A. Zamudio, A.L. Elias, J.A. Rodriguez-Manzo, F. Lopez-Urias, G. Rodriguez-Gattorno, F. Lupo, M. Ruhle, D.J. Smith, H. Terrones, D. Diaz, M. Terrones, Small **2**, 346 (2006)
44. L.Y. Li, Y. Yang, G.L. Yang, X.M. Chen, B.S. Hsiao, B. Chu, J.E. Spanier, C.Y. Li, Nano Lett. **6**, 1007 (2006)
45. B. Kim, W.M. Sigmund, Langmuir **20**, 8239 (2004)
46. Y.C. Xing, J. Phys. Chem. B **108**, 19255 (2004)
47. I. Robel, B.A. Bunker, P.V. Kamat, Adv. Mater. **17**, 2458 (2005)
48. J.H. Chen, G.H. Lu, Nanotechnology **17**, 2891 (2006)
49. G.H. Lu, L.Y. Zhu, P.X. Wang, J.H. Chen, D.A. Dikin, R.S. Ruoff, Y. Yu, Z.F. Ren, J. Phys. Chem. C **111**, 17919 (2007)
50. T. Durkop, S.A. Getty, E. Cobas, M.S. Fuhrer, Nano Lett. **4**, 35 (2004)
51. E.B. Ramayya, D. Vasileska, S.M. Goodnick, I. Knezevic, IEEE Trans. Nanotechnol. **6**, 113 (2007)
52. D. Wang, H. Dai, Appl. Phys. A-Mat. Sci. Process **85**, 217 (2006)
53. A.L. Roest, J.J. Kelly, D. Vanmaekelbergh, E.A. Meulenkamp, Phys. Rev. Lett. **89**, 036801 (2002)
54. R. Konenkamp, Phys. Rev. B **61**, 11057 (2000)
55. M.K. Nazeeruddin, P. Pechy, T. Renouard, S.M. Zakeeruddin, R. Humphry-Baker, P. Comte, P. Liska, L. Cevey, E. Costa, V. Shklover, L. Spiccia, G.B. Deacon, C.A. Bignozzi, M. Gratzel, J. Am. Chem. Soc. **123**, 1613 (2001)
56. P. Wang, S.M. Zakeeruddin, J.E. Moser, M.K. Nazeeruddin, T. Sekiguchi, M. Gratzel, Nat. Mater. **2**, 498 (2003)
57. B.A. Gregg, J. Phys. Chem. B **107**, 4688 (2003)
58. H. Gerischer, Photochem. Photobiol. **16**, 243 (1972)
59. R. Memming, Photochem. Photobiol. **16**, 325 (1972)
60. A. Hagfeldt, M. Gratzel, Acc. Chem. Res. **33**, 269 (2000)
61. M.K. Nazeeruddin, A. Kay, I. Rodicio, R. Humphrybaker, E. Muller, P. Liska, N. Vlachopoulos, M. Gratzel, J. Am. Chem. Soc. **115**, 6382 (1993)
62. D. Cahen, G. Hodes, M. Gratzel, J.F. Guillemoles, I. Riess, J. Phys. Chem. B **104**, 2053 (2000)
63. B. O'Regan, J. Moser, M. Anderson, M. Graetzel, J. Phys. Chem. **94**, 8720 (1990)
64. J. Halme, Master's thesis, Helsinki University of Technology (2002)
65. I. Bedja, S. Hotchandani, P.V. Kamat, J. Phys. Chem. **98**, 4133 (1994)
66. I. Bedja, P.V. Kamat, X. Hua, A.G. Lappin, S. Hotchandani, Langmuir **13**, 2398 (1997)
67. T.W. Hamann, A.B.E. Martinson, J.W. Elam, M.J. Pellin, J.T. Hupp, Adv. Mater. **20**, 1560 (2008)
68. R.W. Fessenden, P.V. Kamat, J. Phys. Chem. **99**, 12902 (1995)
69. K. Vinodgopal, X. Hua, R.L. Dahlgren, A.G. Lappin, L.K. Patterson, P.V. Kamat, J. Phys. Chem. **99**, 10883 (1995)
70. I. Martini, J. Hodak, G.V. Hartland, P.V. Kamat, J. Chem. Phys. **107**, 8064 (1997)
71. A.C. Khazraji, S. Hotchandani, S. Das, P.V. Kamat, J. Phys. Chem. B **103**, 4693 (1999)
72. P.V. Kamat, J. Phys. Chem. **93**, 859 (1989)
73. C. Nasr, P.V. Kamat, S. Hotchandani, J. Phys. Chem. B **102**, 10047 (1998)
74. A. Burke, S. Ito, H. Snaith, U. Bach, J. Kwiatkowski, M. Gratzel, Nano Lett. **8**, 977 (2008)
75. A.C. Fisher, L.M. Peter, E.A. Ponomarev, A.B. Walker, K.G.U. Wijayantha, J. Phys. Chem. B **104**, 949 (2000)
76. T. Oekermann, D. Zhang, T. Yoshida, H. Minoura, J. Phys. Chem. B **108**, 2227 (2004)
77. J. Nelson, Phys. Rev. B **59**, 15374 (1999)
78. J. van de Lagemaat, A.J. Frank, J. Phys. Chem. B **105**, 11194 (2001)
79. K.D. Benkstein, J. van de Lagemaat, N. Kopidakis, A.J. Frank, J. Phys. Chem. B **107**, 7759 (2003)
80. Y.J. Lee, D.S. Ruby, D.W. Peters, B.B. McKenzie, J.W.P. Hsu, Nano Lett. **8**, 1501 (2008)
81. J.M. Macak, H. Tsuchiya, A. Ghicov, P. Schmuki, Electrochem. Commun. **7**, 1133 (2005)
82. R. Hahn, T. Stergiooulus, J.M. Macak, D. Tsoukleris, A.G. Kontos, S.P. Albu, D. Kim, A. Ghicov, J. Kunze, P. Falaras, P. Schmuki, Phys. Status Solidi-Rapid Re. L. **1**, 135 (2007)
83. K. Shankar, J. Bandara, M. Paulose, H. Wietasch, O.K. Varghese, G.K. Mor, T.J. LaTempa, M. Thelakkat, C.A. Grimes, Nano Lett. **8**, 1654 (2008)
84. N. Kopidakis, N.R. Neale, K. Zhu, J. van de Lagemaat, A.J. Frank, Appl. Phys. Lett. **87**, 202106 (2005)
85. R. Beranek, H. Tsuchiya, T. Sugishima, J.M. Macak, L. Taveira, S. Fujimoto, H. Kisch, P. Schmuki, Appl. Phys. Lett. **87**, 243114 (2005)
86. H.J. Snaith, L. Schmidt-Mende, Adv. Mater. **19**, 3187 (2007)
87. P. Brown, K. Takechi, P.V. Kamat, J. Phys. Chem. C **112**, 4776 (2008)
88. K. Shankar, G.K. Mor, A. Fitzgerald, C.A. Grimes, J. Phys. Chem. C **111**, 21 (2007)
89. K. Zhu, T.B. Vinzant, N.R. Neale, A.J. Frank, Nano Lett. **7**, 3739 (2007)
90. S. Nakade, W. Kubo, Y. Saito, T. Kanzaki, T. Kitamura, Y. Wada, S. Yanagida, J. Phys. Chem. B **107**, 14244 (2003)
91. T. Kato, A. Okazaki, S. Hayase, Chem. Commun. 363 (2005)
92. P. Wang, B. Wenger, R. Humphry-Baker, J.E. Moser, J. Teuscher, W. Kantlehner, J. Mezger, E.V. Stoyanov, S.M. Zakeeruddin, M. Gratzel, J. Am. Chem. Soc. **127**, 6850 (2005)
93. M. Gratzel, J. Photochem. Photobiol., A **168**, 235 (2004)
94. P. Brown, P.V. Kamat, J. Am. Chem. Soc. **130**, 8890 (2008)
95. Y. Khalavka, C. Sonnichsen, Adv. Mater. **20**, 588 (2008)
96. A. Kongkanand, K. Tvrdy, K. Takechi, M. Kuno, P.V. Kamat, J. Am. Chem. Soc. **130**, 4007 (2008)
97. W.T. Sun, Y. Yu, H.Y. Pan, X.F. Gao, Q. Chen, L.M. Peng, J. Am. Chem. Soc. **130**, 1124 (2008)
98. K.S. Leschkies, R. Divakar, J. Basu, E. Enache-Pommer, J.E. Boercker, C.B. Carter, U.R. Kortshagen, D.J. Norris, E.S. Aydil, Nano Lett. **7**, 1793 (2007)
99. V.I. Klimov, Appl. Phys. Lett. **89**, 123118 (2006)

100. M.C. Hanna, A.J. Nozik, J. Appl. Phys. **100**, 074510 (2006)
101. S. William, J.Q. Hans, J. Appl. Phys. **32**, 510 (1961)
102. R.H. Baughman, A.A. Zakhidov, W.A. de Heer, Science **297**, 787 (2002)
103. L. Sheeney-Haj-Khia, B. Basnar, I. Willner, Angew. Chem. Int. Ed. **44**, 78 (2005)
104. Q. Huang, L. Gao, Nanotechnology **15**, 1855 (2004)
105. S. Banerjee, S.S. Wong, J. Am. Chem. Soc. **125**, 10342 (2003)
106. S. Banerjee, S.S. Wong, Chem. Commun. 1866 (2004)
107. S. Chaudhary, J.H. Kim, K.V. Singh, M. Ozkan, Nano Lett. **4**, 2415 (2004)
108. J.M. Haremza, M.A. Hahn, T.D. Krauss, Nano Lett. **2**, 1253 (2002)
109. S. Ravindran, S. Chaudhary, B. Colburn, M. Ozkan, C.S. Ozkan, Nano Lett. **3**, 447 (2003)
110. S. Banerjee, S.S. Wong, Nano Lett. **2**, 195 (2002)
111. W.Q. Han, A. Zettl, Nano Lett. **3**, 681 (2003)
112. J.H. Shi, Y.J. Qin, W. Wu, X.L. Li, Z.X. Guo, D.B. Zhu, Carbon **42**, 455 (2004)
113. X.R. Ye, Y.H. Lin, C.M. Wai, J.B. Talbot, S.H. Jin, J. Nanosci. Nanotechnol. **5**, 964 (2005)
114. J.H. Chen, G.H. Lu, L.Y. Zhu, R.C. Flagan, J. Nanopart. Res. **9**, 203 (2007)
115. L.Y. Zhu, G.H. Lu, J.H. Chen, J. Heat Transf.-Trans. ASME **130**, 044502 (2008)
116. J.B. Baxter, A.M. Walker, K. van Ommering, E.S. Aydil, Nanotechnology **17**, S304 (2006)
117. L.E. Greene, M. Law, J. Goldberger, F. Kim, J.C. Johnson, Y.F. Zhang, R.J. Saykally, P.D. Yang, Angew. Chem. Int. Ed. **42**, 3031 (2003)
118. E. Hammel, X. Tang, M. Trampert, T. Schmitt, K. Mauthner, A. Eder, P. Potschke, Carbon **42**, 1153 (2004)
119. J. Wang, R.P. Deo, P. Poulin, M. Mangey, J. Am. Chem. Soc. **125**, 14706 (2003)
120. B. Rajesh, K.R. Thampi, J.M. Bonard, H.J. Mathieu, N. Xanthopoulos, B. Viswanathan, Chem. Commun. 2022 (2003)
121. P.V. Kamat, M. Haria, S. Hotchandani, J. Phys. Chem. B **108**, 5166 (2004)
122. Y. Zhang, S. Iijima, Phys. Rev. Lett. **82**, 3472 (1999)
123. M. Freitag, V. Perebeinos, J. Chen, A. Stein, J.C. Tsang, J.A. Misewich, R. Martel, P. Avouris, Nano Lett. **4**, 1063 (2004)
124. Y.Z. Ma, J. Stenger, J. Zimmermann, S.M. Bachilo, R.E. Smalley, R.B. Weisman, G.R. Fleming, J. Chem. Phys. **120**, 3368 (2004)
125. T. Ando, J. Phys. Soc. Jpn. **66**, 1066 (1997)
126. C.L. Kane, E.J. Mele, Phys. Rev. Lett. **90**, (2003)
127. T.G. Pedersen, Phys. Rev. B **67**, 073401 (2003)
128. P.V. Kamat, Nano Today **1**, 20 (2006)
129. J.Q. Wei, Y. Jia, Q.K. Shu, Z.Y. Gu, K.L. Wang, D.M. Zhuang, G. Zhang, Z.C. Wang, J.B. Luo, A.Y. Cao, D.H. Wu, Nano Lett. **7**, 2317 (2007)
130. L. Tsakalakos, J. Balch, J. Fronheiser, B.A. Korevaar, O. Sulima, J. Rand, Appl. Phys. Lett. **91**, 233117 (2007)
131. B.M. Kayes, H.A. Atwater, N.S. Lewis, J. Appl. Phys. **97**, 114302 (2005)
132. Z.P. Huang, H. Fang, J. Zhu, Adv. Mater. **19**, 744 (2007)
133. K.Q. Peng, Y. Xu, Y. Wu, Y.J. Yan, S.T. Lee, J. Zhu, Small **1**, 1062 (2005)
134. Y.T. Lin, T.W. Zeng, W.Z. Lai, C.W. Chen, Y.Y. Lin, Y.S. Chang, W.F. Su, Nanotechnology **17**, 5781 (2006)
135. J.R. Maiolo, B.M. Kayes, M.A. Filler, M.C. Putnam, M.D. Kelzenberg, H.A. Atwater, N.S. Lewis, J. Am. Chem. Soc. **129**, 12346 (2007)
136. B.M. Kayes, M.A. Filler, M.C. Putnam, M.D. Kelzenberg, N.S. Lewis, H.A. Atwater, Appl. Phys. Lett. **91**, 103110 (2007)